



Effect of surface charge of gold nanoparticles on fluorescence amplification of polydiacetylene-based liposomes

Kyu Ha Park, Sangjin Oh, Jeonghyo Kim, Seung Yun Yang, Beum-Soo An, Dae Youn Hwang, Jae Ho Lee, Hong Sung Kim, Jaebeom Lee & Sungbaek Seo

To cite this article: Kyu Ha Park, Sangjin Oh, Jeonghyo Kim, Seung Yun Yang, Beum-Soo An, Dae Youn Hwang, Jae Ho Lee, Hong Sung Kim, Jaebeom Lee & Sungbaek Seo (2020) Effect of surface charge of gold nanoparticles on fluorescence amplification of polydiacetylene-based liposomes, Journal of Experimental Nanoscience, 15:1, 174-181, DOI: [10.1080/17458080.2020.1761545](https://doi.org/10.1080/17458080.2020.1761545)

To link to this article: <https://doi.org/10.1080/17458080.2020.1761545>



© 2020 The Author(s). Published by Informa UK Limited, trading as Taylor & Francis Group.



[View supplementary material](#)



Published online: 19 May 2020.



[Submit your article to this journal](#)



[View related articles](#)



[View Crossmark data](#)

Effect of surface charge of gold nanoparticles on fluorescence amplification of polydiacetylene-based liposomes

Kyu Ha Park^a, Sangjin Oh^b, Jeonghyo Kim^b , Seung Yun Yang^a, Beum-Soo An^a, Dae Youn Hwang^a, Jae Ho Lee^a, Hong Sung Kim^a, Jaebeom Lee^b and Sungbaek Seo^a 

^aDepartment of Biomaterials Science, Life and Industry Convergence Institute, Pusan National University, Miryang, Republic of Korea; ^bDepartment of Chemistry, Chungnam National University, Daejeon, Republic of Korea

ABSTRACT

Polydiacetylene (PDA)-based liposome have been attractive as sensory platforms owing to their applicability in simultaneous detection of colorimetric and fluorogenic signals. As PDA show low quantum yield, gold nanoparticles (GNPs) were used to amplify the fluorescence of the PDA by localized surface plasmon resonance. In this study, positively and negatively surface charged GNPs at different concentrations were complexed with negatively charged PDA liposome (GNP/PDA). Positively charged GNPs caused tight binding at the surface of negatively charged PDA liposome, became aggregated due to colloidal instability and thereby dramatically quenched the fluorescence of PDA. While negatively charged GNPs sparsely placed on the surface of the PDA liposome, at the optimized complexing condition, generated ~10% of fluorescence amplification compared to non-complexed PDA liposome as observed by the photoluminescence spectra of the stable colloids. Under the optimum incubation conditions, GNP/PDA liposome that specifically binds with Pb^{2+} via its phenolic group, exhibited increased fluorescence intensity compared to the non-complexed PDA liposome-at the same concentration of target Pb^{2+} .

ARTICLE HISTORY

Received 2 September 2019
Accepted 22 April 2020

KEYWORDS

Polydiacetylene sensor; gold nanoparticles; localized surface plasmon resonance

1. Introduction

Polydiacetylene (PDA)-based liposomes are capable of simultaneous detection of colorimetric and fluorogenic signals and hence have been an attractive sensory platform [1–5]. Even though colorimetric signals are easy to observe by the naked eye without the requirement of huge equipment, the liposome solution-based sensing is limited for

CONTACT Sungbaek Seo  sbseo81@pusan.ac.kr  Department of Biomaterials Science, Life and Industry Convergence Institute, Pusan National University, Miryang, 50463, Republic of Korea.

 Supplemental data for this article is available online at <https://doi.org/10.1080/17458080.2020.1761545>.

© 2020 The Author(s). Published by Informa UK Limited, trading as Taylor & Francis Group.

This is an Open Access article distributed under the terms of the Creative Commons Attribution License (<http://creativecommons.org/licenses/by/4.0/>), which permits unrestricted use, distribution, and reproduction in any medium, provided the original work is properly cited.

practical applications, e.g. the colorimetric detection may be interrupted when a colored analyte solution is mixed with it. In these cases, complementary measurements of fluorescence spectra or imaging are required to quantify PDA's fluorogenic transition. The challenge for the fluorogenic sensing of the analyte solution originates from an intrinsic low quantum yield of the PDA [6, 7]. To overcome this shortcoming, amplification of the fluorescence using fluorescence resonance energy transfer (FRET) from donor fluorophore to acceptor PDA [8–10] has been attempted. Although the red emission of FRET-aided PDA liposome was enhanced by external stimuli, i.e. pH change, its practical demonstration to analyte sensing has been not explored. Another commonly used approach to improve fluorescence intensity of fluorophore is through localized surface plasmon resonance (LSPR) by combining the fluorophore with metal nanoparticles [11–13]. This resonance effect depends on the distance between the fluorophore and the metal nanoparticles [14–16]. However, this resonance effect has not been employed to improve fluorescence of PDA, and sensing potential of LSPR-induced amplified sensitivity of PDA liposome has not yet been demonstrated.

Herein, we designed positively and negatively charged gold nanoparticles (GNP) that could interact electrostatically with negatively charged PDA liposome. Colloidal stability of GNP/PDA complex and dispersion/separation distances between GNP and PDA were estimated by dynamic light scattering and electron microscopy, respectively. The LSPR effect of the charged GNP on enhancement or quenching of fluorescence of PDA liposome was evaluated by fluorescence emission spectra. In addition, we investigated the potential of GNP/PDA exhibiting enhanced fluorescence, on increased sensitive detection of lead ion.

2. Experimental details

2.1. Materials and methods

All the solvents were purchased from DAEJUNG Chemicals, Korea. 10,12-Pentacosadiynoic acid (PCDA) was purchased from Alfa Aesar, USA. Dopamine hydrochloride, *N*-(3-dimethylaminopropyl)-*N'*-ethylcarbodiimide hydrochloride, *N*-hydroxysuccinimide, hydrogen tetrachloroaurate(III)trihydrate ($\text{HAuCl}_4 \cdot 3\text{H}_2\text{O}$), cysteamine, sodium borohydride (NaBH_4), gallic acid, and metal powders (FeCl_3 , FeCl_2 , CuCl_2 , ZnCl_2 , and PbCl_2) were purchased from Sigma-Aldrich, USA. Isoflavone was isolated from commercial soybeans. The morphology of the diacetylene (DA) assembly and GNP/DA assembly structures were observed through transmission electron microscope (TEM), H-7600 system (Hitachi, Japan) and scanning electron microscope (SEM), FE-SEM S-4700 (Hitachi, Japan), respectively. The size distribution and zeta potential of the liposome solutions was measured by Zetasizer Nano ZS90 (Malvern Instruments, UK). A hand-held UV lamp (VilberLourmat, France) was used for photopolymerization (254 nm , $1 \text{ mW} \cdot \text{cm}^{-2}$) of PCDA liposomes.

2.2. Preparation of GNP/DA liposome solutions

The PCDA-Dopamine (PCDA-DA) was synthesized as a PCDA derivative in accordance to a previous study [17]. PCDA (3.4 mg, molar eq. 9) and PCDA-DA (0.5 mg, molar eq. 1) were dissolved in $300 \mu\text{L}$ of acetone, and then injected into 20 mL of deionized (DI)water. The suspension was sonicated for 5 min in water bath and cooled for 4 h to obtain a final concentration of 0.5 mM. The liposome solution consisting only of PCDA (3.75 mg)—PCDA liposome solution—was similarly prepared.

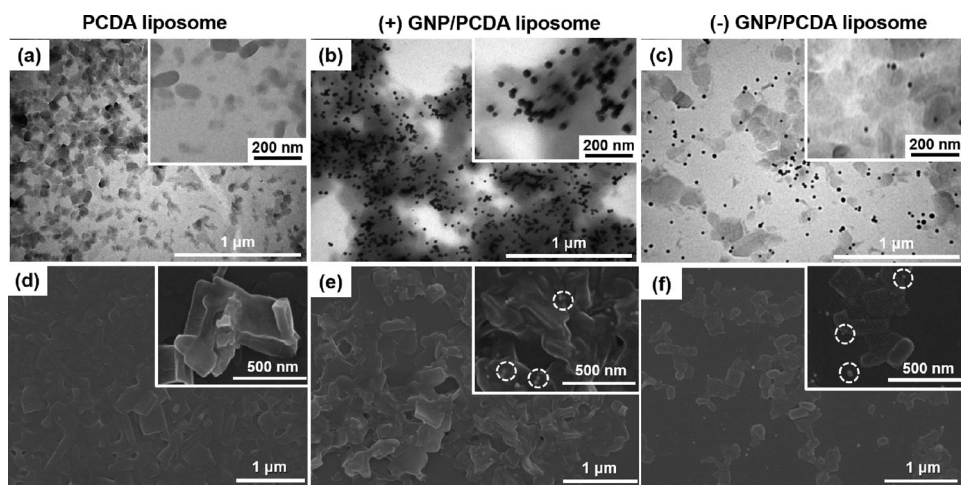


Figure 1. (a)–(c) TEM image and (d–f) SEM image of PCDA liposome, (+) GNP/PCDA liposome, and (–) GNP/PCDA liposome. 2^{-9} dilution of stock (+) GNP (5.16×10^{-12} M) and 2^{-9} dilution of stock (–) GNP (3.34×10^{-12} M) were used for complexing with PCDA liposome. Dotted circles of inset in (e, f) represent GNPs.

The synthesis of the positively charged GNPs has been described in detail elsewhere [18]. The negatively charged GNPs were prepared according to green synthesis method [19] which is briefly described as follows: 10 mg of isoflavone was dissolved in 0.01 M gallic acid solution (10 mL) and the mixture was used as a reducing agent. Subsequently, 300 μL of reducing agent solution was added into 1 mM $\text{HAuCl}_4 \cdot 3\text{H}_2\text{O}$ solution (20 mL) and vigorously stirred for 30 min. The concentration of (+/–) GNPs were calculated according to Haiss's method [20].

The (+) GNP, (–) GNP solution were added into the DA liposome solution, to produce (+) GNP/DA liposome and (–) GNP/DA liposome, respectively.

2.3. UV-Vis absorption, fluorescence emission, and Raman spectrophotometric measurements of GNP/PDA liposome solutions

The UV-Vis absorption spectra of GNP, PDA liposome, and GNP/PDA liposome solutions (200 μL of sample loaded in 96-well plates) were measured by Epoch Microplate Spectrophotometer (BioTek, USA). The fluorescence emission spectra of PDA liposome, and GNP/PDA liposome solutions (2 mL of sample in PSCuvettes) were measured by fluorescence spectrophotometer F-7000 (Hitachi, Japan). The excitation wavelength was set at 470 nm and the fluorescence emission spectra were detected from 500 to 800 nm. The Raman spectra of PDA liposome, and GNP/PDA liposome solutions were measured by Ramboss 500i (Dongwoo Optron Inc., Korea). The range of Raman shift was scanned from 1350 to 2450 cm^{-1} .

3. Results and discussion

We were interested to investigate whether LSPR effect of GNP amplified PDA fluorescence. As the LSPR phenomena depends on the separation distance between the fluorophore and metal nanoparticles [14–16], we hypothesized that the distances in terms of electrostatic interactions (attraction or repulsion) between PDA fluorophore and GNP

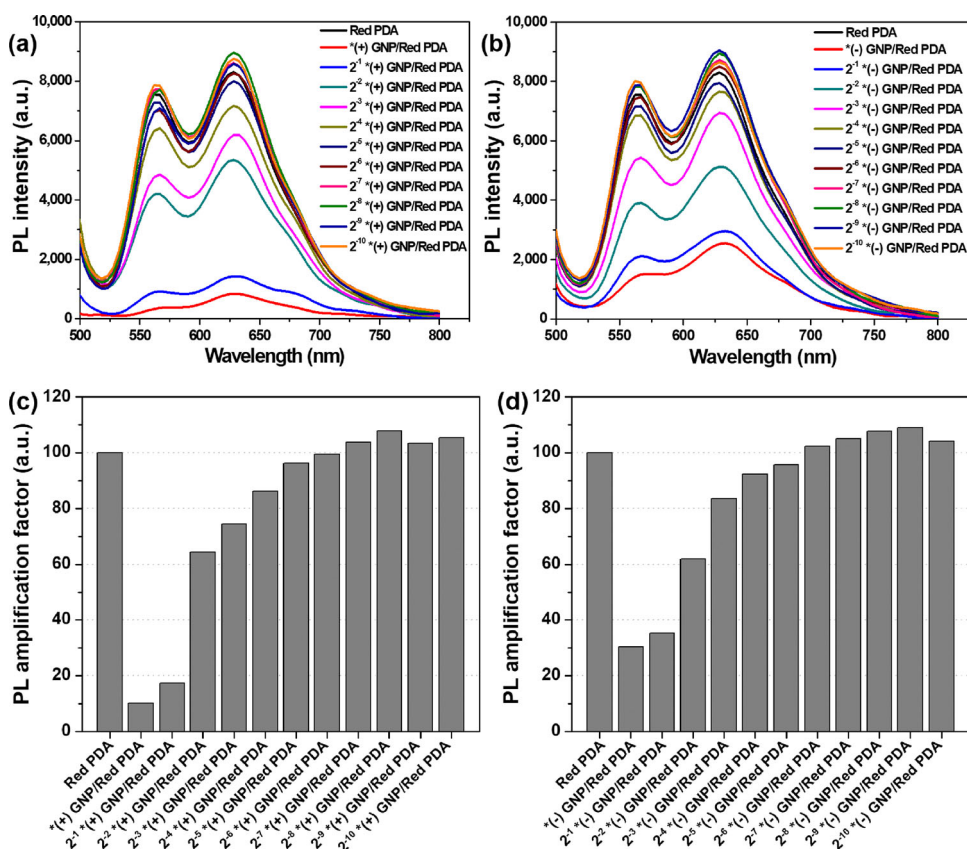


Figure 2. PL spectra of (a) (+) GNP/Red PDA and (b) (-) GNP/Red PDA after addition of diluted GNP solution to Red PDA solution at $\lambda_{\text{ex}} = 470$ nm. *(+) GNP means stock (+) GNP solution of 5.16×10^{-12} M, *(-) GNP means stock (-) GNP solution of 3.34×10^{-12} M. 2^{-x} *GNP states $1/2^x$ dilution of *GNP solution. PL amplification factor is the relative value of transformed PL intensity of each sample at $\lambda_{\text{em}} = 628$ nm, considering PL intensity of pure Red PDA to be 100.

would influence the LSPR effect. We prepared negatively charged PCDA liposome, and positively and negatively charged GNPs. The negatively charged PCDA liposome (-49.0 ± 7.4 mV) exhibited a diameter of 100–200 nm when observed under TEM (Figure 1(a)). The positively charged GNPs (28.5 ± 11.0 mV) of ~ 25 nm diameter were complexed with the PCDA liposome, to produce (+) GNP/PCDA liposome having net charge of -18.0 ± 6.6 mV, showing highly dense complexes as seen in Figure 1(b) (black dot-like shapes represent GNPs and grey cloud-like shapes denote PCDA liposomes). The negatively charged GNPs (-50.5 ± 4.9 mV) of ~ 20 nm diameter were complexed with the PCDA liposome, to produce (-) GNP/PCDA liposome of net charge of -48.0 ± 5.1 mV, showing moderately dispersed complexes as seen in Figure 1(c). The degree of dispersion between GNP and PCDA liposome in the complexes—(+) GNP/PCDA liposome and (-) GNP/PCDA liposome—observed under SEM corresponded to that in the complexes identified by the TEM images (Figure 1(e, f)).

UV-Vis absorption spectra of the complexes exhibited characteristic absorption of both, the PCDA liposome (λ_{abs} of blue phase: 600–650 nm) and the GNPs ($\lambda_{\text{abs, max}} = 524$ nm), indicating that the liposome and GNP coexisted and maintained their own optical properties in the complexes (Figure S1, Supplementary material). The

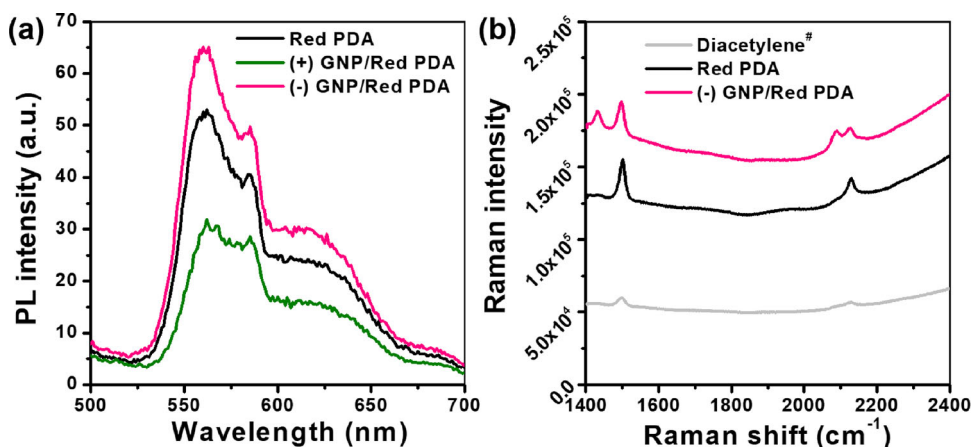


Figure 3. (a) PL spectra of Red PDA, (+) GNP/Red PDA, and (-) GNP/Red PDA 7 days after solution preparation. (b) Raman spectra of Diacetylene[#] (non-photopolymerized PCDA liposome) Red PDA, and (-) GNP/Red PDA. 2^{-8} dilution of stock (-) GNPs were used for complexing with PDA liposome.

characteristic peak of GNPs was shifted to 532 nm in GNP/PCDA liposome, providing evidence of interaction of isolated GNPs to the surface of PCDA liposome [21].

In order to observe the effect of the charged GNP and its concentration on fluorescence of polydiacetylene (PDA), red fluorescent PDA liposome solution (Red PDA) was prepared by pre-heating the photopolymerized solution of the PCDA liposome to 60–70 °C. Serially diluted ($1 \times \sim 2^{-10} \times$) GNP solutions were mixed with 0.5 mM of Red PDA liposome.

Photoluminescence (PL) spectra of the (+) GNP/Red PDA exhibited (+) GNP concentration dependency (Figure 2(a)) with regards to the fluorescence of the Red PDA liposome. In the absence of (+) GNP complex, Red PDA exhibited fluorescence intensity of 8,299 at emission wavelength of 628 nm. When mixed with non-diluted (+) GNP (5.16×10^{-12} M), fluorescence intensity of (+) GNP/Red PDA dropped to 844 (10.2% of fluorescence intensity of pure Red PDA), exhibiting dramatic quenching of PDA fluorescence. It is possibly attributed to that highly dense GNPs placed or disperse with PDA liposomes and induced close proximity-based fluorophore quenching [22, 23]. Another scenario of the fluorophore quenching could be that GNP as a strong quencher plays the role of FRET acceptor in close distance with PDA fluorophore as a donor [24]. Recent study of inserting gold nanoparticles into bilayer of PDA liposome also found that the quenching effect was dominate at high concentration of gold nanoparticle loading [25]. The fluorescence intensity of the (+) GNP/Red PDA gradually increased upon addition of increasingly diluted (+) GNP and exceeded the fluorescence intensity of pure Red PDA in presence of (+) GNP at a dilution of 2^{-7} to 2^{-10} . A maximum fluorescence of 8,957 for (+) GNP/Red PDA was observed upon addition of 2^{-8} dilution of (+) GNP at emission wavelength of 628 nm (Figure 2(c)) (107.9% compared to fluorescence intensity of pure Red PDA). The optimized fluorescence amplification is probably originated from appropriate dispersion/separation distance between GNP and PDA liposome similarly appeared the fluorescence enhancement at moderate distance between metal nanoparticle and fluorophore [11, 12, 14].

PL spectra of (-) GNP/Red PDA were measured after mixing various concentrations of (-) GNP with the Red PDA liposome solution (Figure 2(b)). The fluorescence intensity of

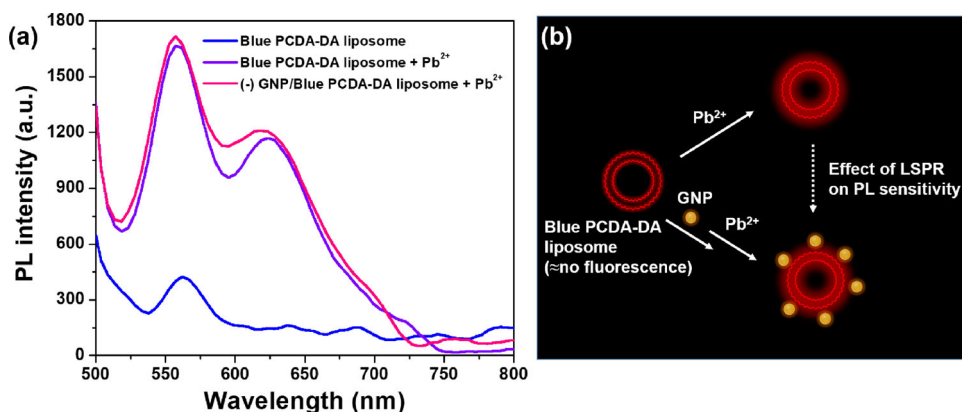


Figure 4. (a) PL spectra of Blue PCDA-DA liposome (before binding to Pb^{2+}), Blue PCDA-DA liposome (after binding to Pb^{2+}) and (-) GNP/Blue PCDA-DA liposome (after binding to Pb^{2+}). (b) Schematic illustration representing effect of localized surface plasmon resonance (LSPR) on photoluminescence (PL) intensity of GNP-induced PCDA-DA liposome as a Pb^{2+} sensing platform.

(-) GNP/Red PDA dropped to 2,523 (30.4% of fluorescence intensity of pure Red PDA), when mixed with non-diluted (-) GNP (3.34×10^{-12} M), showing dramatic quenching of PDA fluorescence, similar to the result of (+) GNP/Red PDA. The fluorescence intensity of the (-) GNP/Red PDA gradually increased upon addition of diluted (-) GNP and surpassed the fluorescence intensity of pure Red PDA at (-) GNP dilution range of $2^{-6} \times$ to 2^{-10} . Maximum fluorescence intensity of 9,043 for the (-) GNP/Red PDA (109.0% compared to the fluorescence intensity of pure Red PDA) was observed at dilution of 2^{-9} (-) GNP (Figure 2(d)). Therefore, $2^{-6} \sim 2^{-10}$ dilutions of (+) GNP/Red PDA and (-) GNP/Red PDA showing enhanced fluorescence compared with the pure Red PDA were used for further studies.

The PL spectra of the GNP/Red PDA liposome solutions were measured again after 7 days to confirm the maintenance of the fluorescence activity. The fluorescence intensity of (+) GNP/Red PDA showed a reduced value compared to that of the Red PDA. This outcome could be attributed to the precipitation of (+) GNP/Red PDA which decreased the red fluorescence (Figure 3(a)). Such precipitation was also visible in various dilutions of (+) GNP/Red PDA, in particular, at higher concentrations of (+) GNP (Figure S2, Supplementary material). We believe that strong electrostatic interactions between (+) GNP and negatively charged Red PDA cause aggregation and colloidal instability. In contrast, the fluorescence intensity of (-) GNP/Red PDA maintained colloidal stability and the enhanced fluorescence compared to that of Red PDA. Raman intensity of (-) GNP/Red PDA was higher than that of pure Red PDA, denoting the Raman signal of PDA (characteristic Raman shift of 1500 cm^{-1} (C=C), 2129 cm^{-1} (C≡C)) was enhanced mainly attributed by surface enhanced Raman scattering of (-) GNP [26, 27] (Figure 3(b)). Thus, (-) GNP/Red PDA could be useful in studying the effect of LSPR to PDA liposome-based sensory platforms, owing to its ability to preserve the enhanced fluorescence property.

To demonstrate the potential of (-) GNP/Red PDA as a sensory platform, we synthesized diacetylene of PCDA derivative (PCDA-Dopamine or PCDA-DA), which is well known to exhibit selective binding towards poisonous Pb^{2+} . Using the PCDA-DA inserted liposome, we confirmed the selectivity of colorimetric transition for Pb^{2+} sensing among various metal ions (Fe^{3+} , Fe^{2+} , Cu^{2+} , Zn^{2+} , Pb^{2+}) (Figure S3, Supplementary material).

We measured fluorescence intensity of just-photopolymerized PCDA-DA liposome solution (Blue PCDA-DA liposome) and (-) GNP/Blue PCDA-DA liposome before and after incubation with Pb^{2+} (0.5 mM). After incubation with Pb^{2+} , the fluorescence intensity of Blue PCDA-DA liposome increased from 424 to 1,653 at emission wavelength of 562 nm (Figure 4(a)). In addition, after incubation with Pb^{2+} , the fluorescence intensity of (-) GNP/Blue PCDA-DA liposome was 1,675 which was 1.3% more than that of Blue PCDA-DA liposome. To our knowledge, this kind of analyte sensing with LSPR-incorporated PDA has not yet been demonstrated. Figure 4(b) illustrates how GNP-moderately bound PDA liposome could enhance red fluorescence of PDA-based sensing platform, thus increasing its sensitivity.

4. Conclusions

To the negatively charged PDA liposome which is broadly utilized as sensory platform, positively charged GNPs were electrostatically attracted and became aggregated. In contrast, negatively charged GNPs moderately bound to the PDA liposome and kept colloidal stability. In range of optimized mixing concentration of (-) GNP, red fluorescence of PDA in (-) GNP/PDA complex was enhanced up to ~10% compared to that of pure PDA attributed to the effect of localized surface plasmon resonance of GNP. Also, it maintained the photoluminescence activity and colloidal stability even after 7 days of sample preparation. The selective detection of Pb^{2+} among the metal ions and a bit improved sensitivity for Pb^{2+} sensing in the GNP/PDA sensory platform were verified.

Author contributions

The manuscript was written through the contributions of all authors. All authors have given approval to the final version of the manuscript.

Disclosure statement

The authors declare no competing financial interest.

Funding

This work was supported by a National Research Foundation of Korea (NRF) grant funded by the Korea government (MSIP: Ministry of Science, ICT & Future Planning) (NRF-2017R1C1B5018327).

ORCID

Jeonghyo Kim  <http://orcid.org/0000-0003-3363-0714>
Sungbaek Seo  <http://orcid.org/0000-0001-5813-4616>

References

1. Ahn DJ, Kim J-M. Fluorogenic polydiacetylene supramolecules: immobilization, micropatterning, and application to label-free chemosensors. *Acc Chem Res.* 2008;41(7):805–816.
2. Lee J, Kim H-J, Kim J. Polydiacetylene liposome arrays for selective potassium detection. *J Am Chem Soc.* 2008;130(15):5010–5011.
3. Lee J, Jun H, Kim J. Polydiacetylene-liposome microarrays for selective and sensitive Mercury(II) detection. *Adv Mater.* 2009;21(36):3674–3677.

4. Kim HN, Guo Z, Zhu W, et al. Recent progress on polymer-based fluorescent and colorimetric chemosensors. *Chem Soc Rev*. 2011;40(1):79–93.
5. Xu Q, Lee S, Cho Y, et al. Polydiacetylene-based colorimetric and fluorescent chemosensor for the detection of Carbon Dioxide. *J Am Chem Soc*. 2013;135(47):17751–17754.
6. Jundt C, Klein G, Moigne JL. Yields of triplet exciton pairs in polydiacetylene films. *Chem Phys Lett*. 1993;203(1):37–40.
7. Olmsted J, Strand M. Fluorescence of polymerized diacetylene bilayer films. *J Phys Chem*. 1983; 87(24):4790–4792.
8. Li X, Matthews S, Kohli P. Fluorescence resonance energy transfer in polydiacetylene liposomes. *J Phys Chem B*. 2008;112(42):13263–13272.
9. Seo S, Kim D, Jang G, et al. Fluorescence resonance energy transfer between polydiacetylene vesicles and embedded benzoxazole molecules for pH sensing. *React Funct Polym*. 2013;73(3): 451–456.
10. Sansee A, Kamphan A, Traiphol R, et al. Embedding luminescent iridium complex into polydiacetylene vesicles as a means of development of responsive luminescent system for imaging applications. *Colloids Surf A Physicochem Eng Asp*. 2016; 497:362–369.
11. Wilson R, Nicolau DV. Separation-free detection of biological molecules based on plasmon-enhanced fluorescence. *Angew Chem*. 2011;123(9):2199–2202.
12. Ray K, Chowdhury MH, Lakowicz JR. Aluminum nanostructured films as substrates for enhanced fluorescence in the ultraviolet-blue spectral region. *Anal Chem*. 2007;79(17):6480–6487.
13. Moula G, Aroca RF. Plasmon-enhanced resonance Raman scattering and fluorescence in Langmuir – Blodgett monolayers. *Anal Chem*. 2011;83(1):284–288.
14. Kühn S, Håkanson U, Rogobete L, et al. Enhancement of single-molecule fluorescence using a gold nanoparticle as an optical nanoantenna. *Phys Rev Lett*. 2006;97(1):17402.
15. Zeng S, Yu X, Law W-C, et al. Size dependence of Au NP-enhanced surface plasmon resonance based on differential phase measurement. *Sens Actuators B Chem*. 2013;176:1128–1133.
16. Osborne SAM, Pikramenou Z. Highly luminescent gold nanoparticles: effect of ruthenium distance for nanoprobe with enhanced lifetimes. *Faraday Discuss*. 2015;185:219–231.
17. Wang D-E, Wang Y, Tian C, et al. Polydiacetylene liposome-encapsulated alginate hydrogel beads for Pb²⁺ detection with enhanced sensitivity. *J Mater Chem A*. 2015;3(43):21690–21698.
18. Oh S, Kim J, Tran VT, et al. Magnetic nanozyme-linked immunosorbent assay for ultrasensitive Influenza A virus detection. *ACS Appl Mater Interfaces*. 2018;10(15):12534–12543.
19. Lee J, Kim HY, Zhou H, et al. Green synthesis of phytochemical-stabilized Au nanoparticles under ambient conditions and their biocompatibility and antioxidative activity. *J Mater Chem*. 2011; 21(35):13316.
20. Haiss W, Thanh NTK, Aveyard J, et al. Determination of size and concentration of gold nanoparticles from UV – Vis spectra. *Anal Chem*. 2007;79(11):4215–4221.
21. Lu W, Wang W, Su Y, et al. Formation of polydiacetylene–NH₂–gold hollow spheres and their ability in DNA immobilization. *Nanotechnology*. 2005;16(11):2582–2586.
22. Malekzad H, Sahandi Zangabad P, Mirshekari H, et al. Noble metal nanoparticles in biosensors: recent studies and applications. *Nanotechnol Rev*. 2017;6(3):301–329.
23. Aslan K, Gryczynski I, Malicka J, et al. Metal-enhanced fluorescence: an emerging tool in biotechnology. *Curr Opin Biotechnol*. 2005;16(1):55–62.
24. Chinen AB, Guan CM, Ferrer JR, et al. Nanoparticle probes for the detection of cancer biomarkers, cells, and tissues by fluorescence. *Chem Rev*. 2015;115(19):10530–10574.
25. Tobias A, Rooke W, Hanks TW. Incorporation of gold nanoparticles into the bilayer of polydiacetylene unilamellar vesicles. *Colloid Polym Sci*. 2019;297(1):85–93.
26. Cui C, Kim S, Ahn DJ, et al. Unusual enhancement of fluorescence and Raman scattering of core-shell nanostructure of polydiacetylene and Ag nanoparticle. *Synth Met*. 2018;236:19–23.
27. Jo SG, Kim BG, Kim J, et al. Waveguiding characteristics of surface enhanced Raman scattering signals along crystalline organic semiconducting microrod. *Opt Express*. 2017;25(6):6215.